



# Toxicity of chlorinated algal-impacted waters: Formation of disinfection byproducts vs. reduction of cyanotoxins

Chao Liu <sup>a, b</sup>, Mahmut S. Ersan <sup>b</sup>, Elizabeth Wagner <sup>c</sup>, Michael J. Plewa <sup>c</sup>, Gary Amy <sup>b</sup>, Tanju Karanfil <sup>b, \*</sup>

<sup>a</sup> Key Laboratory of Drinking Water Science and Technology, Research Center for Eco-Environmental Sciences, Chinese Academy of Sciences, Beijing, 100085, China

<sup>b</sup> Department of Environmental Engineering and Earth Sciences, Clemson University, Anderson, SC, 29625, USA

<sup>c</sup> Department of Crop Sciences, and the Safe Global Water Institute, University of Illinois at Urbana-Champaign, Urbana, IL, 61801, USA

## ARTICLE INFO

### Article history:

Received 29 March 2020

Received in revised form

2 June 2020

Accepted 2 July 2020

Available online 9 July 2020

### Keywords:

Disinfection byproducts

Algal organic matter

Toxicity

Bromide

*Microcystis aeruginosa*

Microcystin

## ABSTRACT

Seasonal algal blooms in surface waters can impact water quality through an input of algal organic matter (AOM) to the pool of dissolved organic matter as well as the release of cyanotoxins. The formation and speciation of disinfection byproducts (DBPs) during chlorination of algal-impacted waters, collected from growth of *Microcystis aeruginosa* were studied. Second-order rate constants for the reactions of microcystins (MCs) with chlorine and bromine were determined. Finally, the toxicity of chlorinated algal-impacted waters was evaluated by Chinese hamster ovary (CHO) cytotoxicity and genotoxicity assays. Under practical water treatment conditions, algal-impacted waters produced less regulated trihalomethanes (THMs) and haloacetic acids (HAAs), haloacetonitriles (HANs), and total organic halogen (TOX) than natural organic matter (NOM). For example, the weight ratios of DBP formation from AOM to NOM (median levels) were approximately 1:5, 1:3, 1:2 and 1:3 for THMs, HAAs, HANs, and TOX, respectively. Increasing initial bromide level significantly enhanced THM and HAN concentrations, and therefore unknown TOX decreased. The second-order rate constant for the reactions of MC-LR (the most common MC species) with chlorine was  $60 \text{ M}^{-1} \text{ s}^{-1}$  at pH 7.5 and  $21^\circ \text{C}$ , and the rate constants for MC congeners follow the order: MC-WR > MC-LW > MC-YR > MC-LY > MC-LR  $\approx$  MC-RR. The reaction rate constant of bromine with MC-LR is two orders of magnitude higher than that of chlorine. Unchlorinated algal-impacted waters were toxic owing to the presence of MCs, and chlorination enhanced their cytotoxicity and genotoxicity due to the formation of toxic halogenated DBPs. However, the toxicity of treated waters depended on the evolution of cyanotoxins and formation of DBPs (particularly unknown or emerging DBPs).

© 2020 Elsevier Ltd. All rights reserved.

## 1. Introduction

The frequent occurrence of blooms of cyanobacteria (also referred to blue-green algae) in freshwater and marine waters worldwide poses a challenge to water supply (Chapra et al., 2017; Paerl and Huisman, 2008). Excretion of algal cells naturally or physico-chemically (e.g., oxidant addition for algae control) during an algal bloom event impacts water quality through the release of bulk algal organic matter (AOM) as well as specific toxic metabolites (e.g., cyanotoxins) (Qi et al., 2016; Xiang et al., 2019).

AOM is characterized by protein, carbohydrate, lipid, and nucleic acid types of structure (Henderson et al., 2008; Her et al., 2004). Due to its hydrophilic character and low aromaticity, it is expected that this hydrophilic organic carbon fraction is recalcitrant to coagulation (Lee and Westerhoff, 2006; Widrig et al., 1996), which is different from terrestrial natural organic matter (NOM) derived from lignin and containing a mainly polyphenolic structure (Leenheer and Croué, 2003). Therefore, the fraction of AOM over the bulk dissolved organic matter (DOM) may increase after a conventional treatment train.

When compared with bulk AOM, cyanotoxins are present at much lower levels (in the range of  $\mu\text{g/L}$ ). Among various identified cyanotoxins, microcystins (MCs) have received the most concern due to their occurrence and high toxicity in waters (Xiang et al.,

\* Corresponding author.

E-mail address: [tkaranfil@clemson.edu](mailto:tkaranfil@clemson.edu) (T. Karanfil).

2019). They are monocyclic heptapeptides generated by non-ribosomal peptide synthetases, produced by species of freshwater cyanobacteria, primarily *Microcystis aeruginosa*. The common structure of MCs (Table S1, supplementary material) is cyclo(-d-Ala-L-X-d-erythro- $\beta$ -methylAsp (iso-linkage)-L-Z-Adda-d-Glu(iso-linkage)-N-methyldehydroAla) where Adda stands for the unique  $\alpha$ -amino acid 3-amino-9-methoxy-2,6,8-trimethyl-10-phenyldeca-4(E),6(E)-dienoic acid (Rinehart et al., 1988). To date, more than 100 different congeners have been reported. Among them, the most common MC congeners are MC-RR, -YR, -LR, -WR, -LY, and -LW, which have combinations of the following  $\alpha$ -amino acids in the X and Y positions: arginine (Arg, R), leucine (Leu, L), tryptophan (Trp, W), and tyrosine (Tyr, Y). MCs known as potent hepatotoxins and tumor promoters express their toxicity by inhibiting protein phosphatases activity (Dawson, 1998; Yoshizawa et al., 1990). MC-LR is the most toxic MC variant, with an LD<sub>50</sub> (median lethal dose) value of 50 mg/kg (Dawson, 1998). Due to its acute toxicity, the World Health Organization has set a provisional drinking water guideline value of 1  $\mu$ g/L for MC-LR (World Health Organization, 2011).

Chlorine disinfection after conventional treatment is commonly used to provide hygienically safe drinking water. However, chlorine (in the form of hypochlorous acid, i.e., HOCl, in water) can react with DOM to produce toxic disinfection byproducts (DBPs) (Liu et al., 2017). The most recognized DBPs formed during chlorination are trihalomethanes (THMs) and haloacetic acids (HAAs), which are currently regulated by the United States Environmental Protection Agency (US EPA) as the maximum contaminant levels (MCLs) for the sum of four THMs and five HAAs in drinking water at 80  $\mu$ g/L and 60  $\mu$ g/L, respectively (U.S. Environmental Protection Agency, 2006). Although concentrations of unregulated DBPs, such as haloacetonitriles (HANs), and halonitromethanes (HNMs), in drinking waters were reported at much lower levels than those of regulated THMs and HAAs, the toxicity risk posed by these unregulated DBPs is higher (Plewa et al., 2017).

Bromide ( $\text{Br}^-$ ) is ubiquitous in source waters, with highly variable levels in a range of <10 to >1000  $\mu$ g/L (Liu et al., 2012). The usage of desalinated seawaters, seawater intrusion, and anthropogenic activities such as hydraulic fracturing and coal-fired power plants lead to elevated  $\text{Br}^-$  levels (Good and VanBriesen, 2016; Kim et al., 2015). During chlorination process,  $\text{Br}^-$  can be oxidized to hypobromous acid (HOBr), which can react with DOM to form brominated DBPs (Br-DBPs). The formation of Br-DBPs is of particular concern since they are more cytotoxic and genotoxic than their chlorinated analogues (Plewa et al., 2004; Wagner and Plewa, 2017).

Due to the release of AOM and cyanotoxins during seasonal algal bloom events impacting water quality, chlorination may bring *pros* and *cons* to the toxicity of treated waters. It was reported that, compared with NOM, AOM could form significant amounts of nitrogenous DBPs upon chlorination under formation potential (FP) conditions where high initial concentrations of chlorine and longer reaction time were employed (Fang et al., 2010). However, the comparative formation of DBPs formed from AOM and NOM under realistic drinking water treatment conditions remains unknown.

On the other hand, during seasonal algal bloom events, concentrations of MCs can be much higher than the regulation (1.0  $\mu$ g/L). For example, a maximum concentration of MCs in lake waters of Finland was reported as 42  $\mu$ g/L (Spoof et al., 2003). Conventional coagulation-sedimentation-filtration treatment processes showed poor removal of MCs (Himberg et al., 1989), while MC variants (e.g., MC-LR, -RR, and -YR) can be degraded by chlorine (Acero et al., 2005; Ho et al., 2006; Merel et al., 2010). This indicates the opportunity for optimization of chlorine disinfection/oxidation process to control MCs. In the presence of  $\text{Br}^-$ , it was reported that the

secondarily formed HOBr has higher reactivity towards phenols than chlorine (Heeb et al., 2014). However, the role of  $\text{Br}^-$  in the degradation of cyanotoxins is not clear. Given the complex role of chlorination in determining the toxicity of treated algal-impacted waters, the experimental measurement of cytotoxicity and genotoxicity is required to decipher the forcing agent (formation of halogenated DBPs vs. degradation of cyanotoxins) for the toxicity.

In view of increasing occurrence of harmful algal bloom in surface waters, the objectives of this study were (1) to investigate the comparative formation of DBPs during chlorination of algal-impacted waters and surface waters under practical water treatment conditions, (2) to study the kinetics for the reactions of MCs with chlorine and bromine, and (3) to determine the mammalian cell cytotoxicity and genotoxicity of the extracted organics of the chlorinated water samples.

## 2. Materials and methods

### 2.1. Reagents, culturing of cyanobacteria, and preparation of algal-impacted waters

All chemical solutions were prepared from reagent grade chemicals or stock solutions using deionized Milli-Q (MQ) water (18.2 M $\Omega$ -cm, Millipore). The descriptions of all other standards and reagents used in this study are provided in Text S1 of the supplementary material.

*Microcystis aeruginosa*, which was identified as the main species responsible for severe harmful blooms of cyanobacteria in large lakes worldwide (Liu et al., 2019), was selected as the model cyanobacterium species in this study. The culturing of cyanobacteria and preparation of algal-impacted waters are described in our previous study (Liu et al., 2018), which is further detailed in Text S2 of the supplementary material. In addition, six types of raw surface waters and treated waters (after coagulation and sand filtration but without disinfection) were collected from several water treatment plants in South Carolina, USA. The selection of these waters was based on their distinct specific ultraviolet absorbance (SUVA, indicator of aromatic and hydrophobic properties) values ranging from 1.7 to 5.1 L/mg-m, covering the typical SUVA values of surface waters in water treatment. Additional information regarding sampling and water characteristics can be found in supplementary material (Text S3 and Table S2, respectively).

### 2.2. Analytical methods

Four THMs (chloroform (TCM), bromodichloromethane (BDChM), dibromochloromethane (DBChM), and bromoform (TBM)), six HANs (monochloro-, dichloro-, trichloro-, monobromo-, dibromo-, and bromochloro-acetonitrile (CAN, DCAN, TCAN, BAN, DBAN, and BCAN, respectively), and nine HAAs (i.e., HAA9, sum of monochloro-, dichloro-, trichloro-, monobromo-, dibromo-, bromochloro-, bromodichloro-, dibromochloro-, and tribromo-acetic acids (MCAA, DCAA, TCAA, MBAA, DBAA, BCAN, BDCAA, DBCAA, and TBAA, respectively)), were quantified. Detailed information on analytical methods of total dissolved organic carbon (DOC), total dissolved nitrogen, concentrations of residual chlorine, anions, total organic halogen (TOX), and DBPs can be found in Text S4 of supplementary material. The measurement of MCs (MC-RR, -YR, -LR, -WR, -LY, and -LW) was detailed in Text S5 of supplementary material.

### 2.3. Reaction rate constants of microcystins with chlorine and bromine

The kinetics for the MC reactions with chlorine and bromine

were determined at pH 7.5 (10 mM phosphate buffer) and 21 °C (room temperature) in Milli-Q water under pseudo-first-order conditions where chlorine or bromine was at least 10-fold in excess. Bromine solutions were prepared by the reaction of chlorine with Br<sup>-</sup> according to a previously described method (Liu et al., 2012). The reaction was initiated by injecting 50 µL of the chlorine (or bromine) stock solution into 5 mL of solutions containing MCs which were capped with PTFE-faced silica septum. After the addition of oxidant, the vials were placed on a vortex mixer with stirring for 10 s. Samples (300 µL) were transferred into vials with inserts containing 10 µL of sodium sulfite solutions (50 mM) to quench the oxidant. Afterwards, concentrations of residual MCs were analyzed directly by HPLC. All experiments were duplicated.

#### 2.4. Experiments for chlorination of algal-impacted waters and surface waters

For chlorination of algal-impacted waters, experiments were conducted in ~6 L of capped bottles since large volume was needed for toxicity measurement. For chlorination of surface waters, experiments were carried out in 250 mL of capped amber bottles. All experiments were performed under headspace-free conditions at pH 7.5 in the dark at room temperature (21 ± 1 °C). Each source water (DOC = 2 mg/L) in the presence of various initial Br<sup>-</sup> concentrations (i.e., 0–800 µg/L, covering the typical Br<sup>-</sup> range in source waters) was treated with chlorine under practical water treatment conditions (4 mg/L Cl<sub>2</sub>, for 24 h). Reactions were initiated by the injection of an aliquot of an HOCl stock solution. After 24 h, 240 mL of water samples were withdrawn, and after the measurement of residual oxidants the corresponding amount of ascorbic acid (molar ratio = 1.0) was added to quench the residual for the DBP analyses. Ascorbic acid was recommended for the quenching of water samples for the analyses of organic DBPs (i.e., THMs, HAAs, HANs, etc), since it does not decompose these DBPs (Kristiana et al., 2014). The remaining chlorinated algal-impacted waters were extracted for mammalian cell toxicity experiments.

#### 2.5. Isolation of organics

The organics resulting from unchlorinated (used as the control) and chlorinated algal-impacted waters were concentrated by adsorption onto XAD resins (Plewa, 2016). XAD-2 (Amberlite XAD 2, Sigma Aldrich, MO) and XAD-8 (Supelite DAX 8, Sigma Aldrich, MO) resins were pre-cleaned in a Soxhlet extractor and stored in pure methanol in the refrigerator before use. A slurry of 55 mL XAD-2/XAD-8 resin mix (measured in a graduated cylinder) was packed on a plug of glass wool in a glass chromatography column. The water samples were acidified to pH < 2 by sulfuric acid prior to being added into the column for extraction, to ensure the protonation of carboxylic organics. The resins were eluted with 400 mL of optima spectroscopy grade ethyl acetate (Fisher Scientific, PA) to elute the organic compounds. The residual water in the ethyl acetate eluent was removed using a separatory funnel, followed by passing the hydrophobic fraction through a column of anhydrous sodium sulfate. The ethyl acetate extract was then reduced to 1–1.5 mL by a rotary evaporator at 50–60 °C and evaporated blown down to a sludge using a gentle stream of nitrogen gas. For each sample, dimethyl sulfoxide (DMSO) was used to dissolve the organic extract, resulting in a 10<sup>5</sup>-fold concentration of organic compounds derived from the water samples.

#### 2.6. Chinese hamster ovary (CHO) cells

The CHO cells, cell line AS52, clone 11-4-8 were used for the mammalian cell toxicity studies and maintained in Ham's F12 + 5%

fetal bovine serum (FBS) medium at 37 °C in a humidified atmosphere of 5% CO<sub>2</sub>. The cells exhibit normal morphology, express cell contact inhibition and grow as a monolayer without expression of neoplastic foci.

#### 2.7. CHO cell chronic cytotoxicity assay

The CHO cell microplate chronic cytotoxicity assay measures the reduction in cell density as a function of the concentration of the test agent during a 72-h exposure period. The detailed procedure is presented in Text S6 of supplementary material. Briefly, the protocol involved the use of a 96-well flat-bottomed micro-plate to evaluate the diluted organic extracts of the algal-impacted water samples with varying concentration factors. For each concentration factor of a given water sample, 4–8 replicates were analyzed and the experiments were repeated. The data were used to generate a concentration-response curve for each algal-impacted water sample. Regression analysis was applied to calculate the LC<sub>50</sub> defined as the calculated concentration of the test agent that induced a cell density that was 50% of the negative control. The metric for the aqueous or organic concentration was the concentration factor, which allows for direct comparison among the water samples.

#### 2.8. CHO cell single cell gel electrophoresis assay

Single cell gel electrophoresis (SCGE, comet) is a molecular genetic assay that can quantitatively measure the level of genomic DNA damage induced in individual nuclei of cells (Fairbairn et al., 1995; Rundell et al., 2003; Tice et al., 2000; Wagner and Plewa, 2009). A flow diagram of the SCGE procedure is presented in Fig. S1 of supplementary material, and the detailed procedure is provided in Text S7 of supplementary material. Akin to CHO chronic cytotoxicity assay, 4 × 10<sup>4</sup> CHO cells were added to each microplate well and treated with a series of diluted organic extracts of the algal-impacted water samples with varying concentration factors for 4 h. Experiments were repeated 2–3 times for each water sample concentrate. A computerized image analysis system (Comet IV, Perspective Instruments, Ltd, Suffolk, UK) was employed to determine the %Tail DNA (the amount of DNA that migrated from the nucleus into the microgel) of the nuclei as the measure of DNA damage (Kumaravel and Jha, 2006). The digitalized data (Fig. S2 of supplementary material) were automatically transferred to a computer-based spreadsheet for subsequent statistical analysis. For concentration factors of each algal-impacted water sample with the cell viability > 70%, a concentration-response curve was generated. Based on the regression analysis for the curve fitting, the concentration factor that induced a 50%Tail DNA value was calculated.

#### 2.9. Statistical analyses

For the cytotoxicity and genotoxicity assays the units of measure were the clone of exposure cells and the microgel, respectively. A one-way analysis of variance (ANOVA) test was conducted to determine if each water sample induced a statistically significant level of either cytotoxicity or genotoxicity within the concentration response curve. If a significant *F* value (*P* ≤ 0.05) was obtained, a Holm-Sidak multiple comparison versus the control group analysis was performed to identify the lowest cytotoxic or genotoxic concentration factor. The power of the test statistic (1-β) was maintained as ≥ 0.8 at α = 0.05. To determine significant differences among the water sample groups, a bootstrap statistical approach was used to generate a series of multiple LC<sub>50</sub> values and multiple 50%Tail DNA values for each water sample. For each LC<sub>50</sub> value, a cytotoxicity index (CTI) value was calculated as (LC<sub>50</sub><sup>-1</sup>)(10<sup>3</sup>). For the 50% Tail DNA values a genotoxicity index (GTI) value was calculated

(50% Tail DNA<sup>-1</sup>)(10<sup>3</sup>). These CTI and GTI values were separately analyzed using an ANOVA test.

### 3. Results and discussion

#### 3.1. Comparative formation of DBPs from algal-impacted waters and surface waters

##### 3.1.1. THMs

Fig. 1 presents the concentrations of measured THMs from algal-impacted waters and surface waters in the presence of various initial Br<sup>-</sup> concentrations. Concentrations of THMs from algal-impacted waters ranged from 6.2 (±0.7) (representing mean±standard errors in this paper) to 18.1 (±0.5) µg/mgC for initial Br<sup>-</sup> concentrations of 40–800 µg/L. In contrast, median concentrations of those from surface waters (where NOM predominates) were in the range of 33.9–98.3 µg/mgC. These results indicate that the formation of THMs from AOM is much lower than that of comparable NOM. For example, the median THM concentration from NOM was as five times high as that formed from AOM at initial Br<sup>-</sup> concentration of 40 µg/L. It was reported that TCM concentration in the absence of Br<sup>-</sup> under FP conditions from Suwannee River NOM was almost twice that from AOM (i.e., c.a. 70 vs 30 µg/mgC) (Fang et al., 2010). Therefore, the gap for the THM formation from NOM vs AOM is smaller under FP conditions. NOM is typically comprised of >50% of humic substances which contain aromatic/phenolic and carboxyl group contents, functioning as fast reacting THM precursors (Leenheer and Croué, 2003; Liu and Croué, 2016). However, humic substances only account for 14%–22% of the total DOC in AOM and the major fraction is protein and carbohydrate type of structure which might be slow-reacting THM precursors (Liu et al., 2018). Therefore, the quantification of THM formation for AOM under FP conditions may not represent the THM formation for practical applications where low chlorine dose and short reaction time were employed.

It was seen that increasing the initial Br<sup>-</sup> concentration increased the formation of total THMs from AOM and NOM (Fig. 1). For example, median THM concentrations from NOM were 33.9,

48.8, 69.7, and 98.3 µg/mgC for initial Br<sup>-</sup> concentrations of 40, 200, 400, and 800 µg/L, respectively. This is in line with previous studies (Ersan et al., 2019a; Hu et al., 2010; Hua et al., 2006). In addition, increasing initial Br<sup>-</sup> concentration shifted the formation of THMs from chlorinated to brominated species.

##### 3.1.2. HAAs

Fig. 2 shows that total concentrations of HAAs formed from algal-impacted waters ranged from 8.0 ± 0.4 to 11.3 ± 0.3 µg/mgC, while median concentrations of those from surface waters were in the range of 33.6–54.6 µg/mgC. Similar to THM, the major fraction of NOM is aromatic/phenolic and carboxyl groups which are HAA precursors (Leenheer and Croué, 2003). Therefore, the median concentration of HAAs formed from NOM was three times as high as that of AOM at initial Br<sup>-</sup> concentration of 40 µg/L. Different from THM, increasing initial Br<sup>-</sup> concentration only slightly increased total concentrations of HAAs formed from AOM. However, the speciation of HAAs was shifted from chlorinated species to brominated analogues. All nine HAA species were measured, and their concentrations vary with the change in the initial Br<sup>-</sup> concentration.

##### 3.1.3. HANs

The formed total HANs from AOM are present at slightly lower concentrations than their median concentrations from NOM (e.g., 1.7 vs. 2.3 µg/mgC at initial Br<sup>-</sup> concentration of 40 µg/L) (Fig. 3). HANs were formed from nitrogen-containing functional groups, such as amines, amino acids which are derived from proteins, and/or anthropogenic compounds (Hureiki et al., 1994). Nevertheless, their precursors are structure specific. For example, the DCAN formation yield from aspartic acid was two orders of magnitude higher than those from other amino acids (e.g., glycine, alanine, etc) (Selbes et al., 2015). It is likely that the surface waters have more HAN precursors than algal-impacted water harvested in this study. Due to the distinct precursor of HANs versus THM/HAA formed from aromatic/phenolic and carboxyl groups, the ratio of HAN formation from NOM to HAN formation from AOM was 1.3–1.6, which is much smaller than that of THM/HAA (3.0–5.0). Although

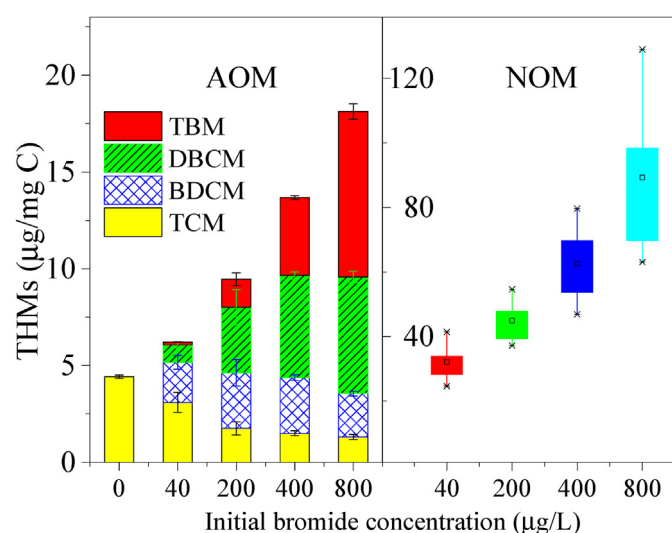


**Fig. 1.** Comparative formation of THMs during chlorination of AOM and NOM in the presence of various initial bromide concentrations. Experimental conditions: [HOCl]<sub>0</sub> = 4 mg/L, [Br<sup>-</sup>]<sub>0</sub> = 0–800 µg/L, [DOC] = 2.0 mg C/L, pH = 7.5, T = 21 ± 1 °C, reaction time = 24 h. For the NOM, the box shows the 25th and 75th percentile. The whisker denotes the 5th and 95th percentile. The symbols “\*” and “□” represent outliers and mean values, respectively.

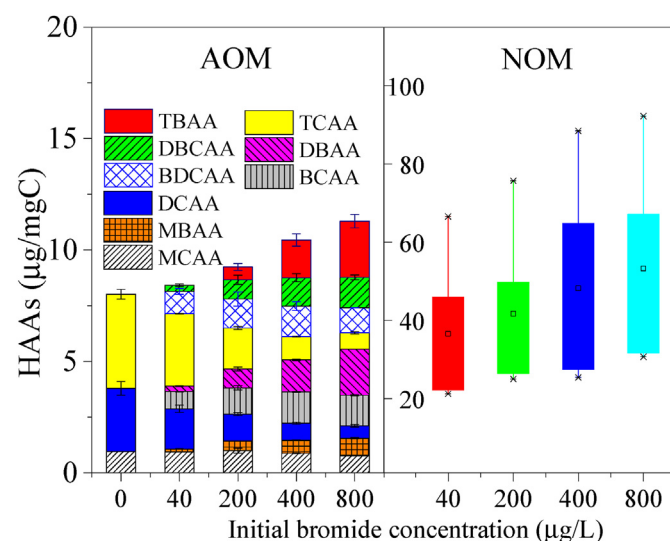


**Fig. 2.** Comparative formation of HAAs during chlorination of AOM and NOM in the presence of various initial bromide concentrations. Experimental conditions: [HOCl]<sub>0</sub> = 4 mg/L, [Br<sup>-</sup>]<sub>0</sub> = 0–800 µg/L, [DOC] = 2.0 mg C/L, pH = 7.5, T = 21 ± 1 °C, reaction time = 24 h. For the NOM, the box shows the 25th and 75th percentile. The whisker denotes the 5th and 95th percentile. The symbols “\*” and “□” represent outliers and mean values, respectively.



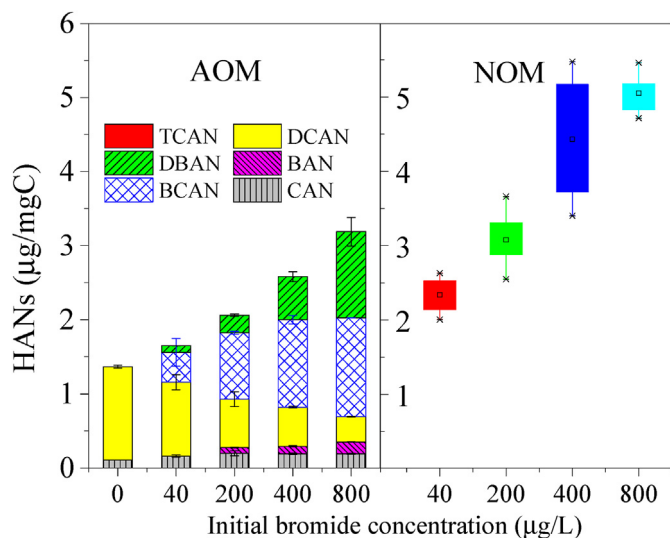


**Fig. 3.** Comparative formation of HANs during chlorination of AOM and NOM in the presence of various initial bromide concentrations. Experimental conditions:  $[\text{HOCl}]_0 = 4 \text{ mg/L}$ ,  $[\text{Br}^-]_0 = 0\text{--}800 \text{ µg/L}$ ,  $[\text{DOC}] = 2.0 \text{ mg C/L}$ ,  $\text{pH} = 7.5$ ,  $T = 21 \pm 1 \text{ °C}$ , reaction time = 24 h. For the NOM, the box shows the 25th and 75th percentile. The whisker denotes the 5th and 95th percentile. The symbols "\*" and "□" represent outliers and mean values, respectively.

AOM does not appear to be an important THM/HAA precursor, it can form comparable levels of HANs with NOM.

Increasing the initial  $\text{Br}^-$  concentration significantly increased concentrations of total HANs from AOM and NOM. For example, increasing the initial  $\text{Br}^-$  concentration from 0 to 800  $\text{µg/L}$  almost doubled the concentrations of total HANs, indicating that bromine favours the formation of HANs, as compared to chlorine. This may increase the toxicity of treated waters since brominated HANs are much more toxic than their chlorinated analogues (Wagner and Plewa, 2017).

### 3.1.4. TOX

The formation of TOX, total organic chlorine (TOCl), and total organic bromine (TOBr) during chlorination of AOM and NOM is presented in Fig. 4. AOM produced lower TOX (ca. 49  $\text{µg Cl/mgC}$ ) than their median levels from NOM (128.0–141.5  $\text{µg Cl/mgC}$ ). In addition, concentrations of TOX remained generally stable irrespective of changes in initial  $\text{Br}^-$  concentrations since there was no change for the amounts of precursors. Nevertheless, increasing initial  $\text{Br}^-$  concentrations shifted the formation of TOX from chlorinated species to brominated analogues.

Fig. S3 of supplementary material shows the fraction of each group of DBP of total TOX from chlorination of algal-impacted waters. THM and HAA are the main groups of DBPs, while HAN is the minor species. Unknown TOX which was calculated from the difference between the TOX and the sum of halogen-equivalent concentrations of measured specific DBPs accounted for >70% of total TOX due to the hydrophilic nature of AOM. In contrast, for NOM, unknown TOX only accounts for 50–60% of the total TOX (Fig. S4 of supplementary material). This may be attributed to NOM being more aromatic and hydrophobic (as indicated by higher SUVA values in Table S2 of supplementary material), forming more known DBPs (Henderson et al., 2008; Liu et al., 2018). Generally increasing the initial  $\text{Br}^-$  concentration decreased the percentage of unknown TOX, indicating that the formation of known DBPs (e.g., THM) was favoured in the bromination process.

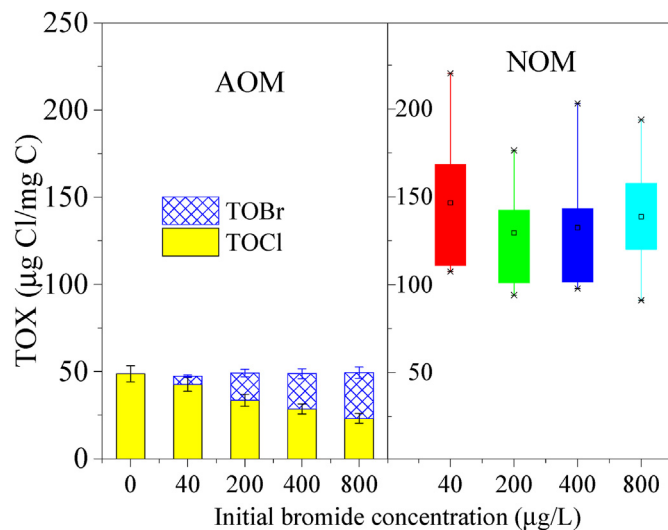


**Fig. 4.** Comparative formation of TOX during chlorination of AOM and NOM in the presence of various initial bromide concentrations. Experimental conditions:  $[\text{HOCl}]_0 = 4 \text{ mg/L}$ ,  $[\text{Br}^-]_0 = 0\text{--}800 \text{ µg/L}$ ,  $[\text{DOC}] = 2.0 \text{ mg C/L}$ ,  $\text{pH} = 7.5$ ,  $T = 21 \pm 1 \text{ °C}$ , reaction time = 24 h. For the NOM, the box shows the 25th and 75th percentile. The whisker denotes the 5th and 95th percentile. The symbols "\*" and "□" represent outliers and mean values, respectively.

### 3.2. Kinetics for the reactions of microcystins with chlorine or bromine

Even though toxic halogenated DBPs can be formed during chlorination, chlorine can react with the cyanotoxins in algal-impacted waters. Previous studies have shown that the reaction of MCs with chlorine is of second-order in total, first-order in oxidant (chlorine) and first-order in MCs (Acero et al., 2005; Rodriguez et al., 2007). The rate constant for the reaction of chlorine/bromine with MCs was investigated under pseudo-first-order conditions (i.e., at least a 10:1 molar ratio of oxidant to MCs) in a batch reactor. Fig. S5 of supplementary material shows the degradation of various MCs by chlorination and bromination (only for MC-LR). Almost 90% of initial MC-LR was degraded by chlorine in 30 min, and complete degradation by bromine was achieved in 0.5 min. This indicated that bromine reacts much faster than chlorine toward MC-LR. For other MCs, over 95% of degradation was seen in 15 min. The degradation rates follow the order: MC-WR > MC-LW > MC-YR > MC-LY > MC-RR. To determine the second order rate constants for the reactions of oxidant with MCs, the reaction can be written as:



and hence the rate of MC degradation can be expressed as:

$$-d[\text{MC}]/dt = k_{\text{app}}[\text{MC}][\text{HOCl}] \quad (2)$$

where  $k_{\text{app}}$  is the apparent second-order rate constant. Under the pseudo-first-order conditions, Equation (2) is simplified to:

$$-d[\text{MC}]/dt = k'[\text{MC}] \quad (3)$$

and

$$k' = k_{\text{app}}[\text{HOCl}]_0 \quad (4)$$

Taking natural log at both sides of Equation (3) gives:

$$\ln([MC]/[MC]_0) = -k't \quad (5)$$

where  $k'$  is the pseudo-first-order rate constant. Therefore, if the assumption of first-order kinetics with respect to MCs is correct, the plot of the  $\ln([MC]/[MC]_0)$  versus time should yield a straight line for each experiment, and the slope is  $k'$ , as shown in Fig. S6 of supplementary material.

Table S3 of supplementary material summarizes the values of  $k'$  obtained for various MCs. Based on the obtained  $k'$  and Equation (4), second-order rate constants for the reactions of MCs with chlorine or bromine can be deduced, as shown in Table 1. The reaction rate constants of MCs vary, depending on the connected L-amino acids in the X and Y positions and the oxidant (chlorine or bromine). For example, the second-order rate constant for the reaction between chlorine and MC-LR is  $60 \text{ M}^{-1}\text{s}^{-1}$  at pH 7.5 and  $21^\circ\text{C}$ , which was similar to  $61.8 \text{ M}^{-1}\text{s}^{-1}$  reported in literature (Acero et al., 2005). MC-RR shows similar reactivity ( $k = 58.6 \text{ M}^{-1}\text{s}^{-1}$ ) with MC-LR. Higher reaction constants ( $k = 92.8$  and  $138.6 \text{ M}^{-1}\text{s}^{-1}$ ) were determined for MC-LY and MC-YR, respectively. This might be due to their tyrosine (denoting to "Y" in the name) in which the phenolic moiety is the reactive site for chlorine (Deborde and von Gunten, 2008). MC-LW and MC-WR are highly reactive, >90% of initial MC-LW and MC-WR was degraded in 1 min. Therefore, it is difficult to withdraw multiple samples in a batch reactor during such a short period to accurately determine the  $k'$ . However, based on the available data sampled in the short time, the range of  $k'$  can be approximated. As a result, the range of  $k$  for MC-LW and MC-WR is  $\geq 371$  and  $\geq 1214 \text{ M}^{-1}\text{s}^{-1}$ , respectively. Their greater reaction rate constants than other MCs are likely due to a tryptophan moiety (denoting to "W" in the name) being highly reactive towards chlorine (Pattison et al., 2007).

Interestingly, bromine reacts much faster than chlorine with MC-LR, and >95% of MC-LR was degraded by bromine in 0.5 min. Likewise, the range of  $k$  is  $\geq 6350 \text{ M}^{-1}\text{s}^{-1}$ , indicating that the second-order reaction rate constant of bromine with MC-LR is two orders of magnitude higher than that of chlorine. The reactions between bromine and other MCs were not studied due to the difficulty in measuring the fast reactions (completed in 1 min), but based on the order of the second-order rate constants for the reactions between chlorine and MCs, it can be expected that the  $k$  for the reactions between bromine and other MCs is  $\geq 6350 \text{ M}^{-1}\text{s}^{-1}$ . It has been recognized that bromine reacts with phenolic compounds much faster than chlorine (factor of  $\sim 3000$ ) (Heeb et al., 2014). Apparently, the presence of  $\text{Br}^-$  during chlorination of algal-impacted waters will promote the degradation of MCs.

### 3.3. CHO cell chronic cytotoxicity analyses

Chlorination can be used to destruct cyanotoxins in a seasonal harmful algal bloom event, but this could increase the formation of toxic halogenated DBPs. Therefore, the impact of chlorination on

**Table 1**  
Second-order rate constants for reactions of microcystins with chlorine or bromine (pH = 7.5, T =  $21 \pm 1^\circ\text{C}$ ).

Compounds	$k_{\text{HOCl}} (\text{M}^{-1}\text{s}^{-1})^a$	$k_{\text{HOCl}} (\text{M}^{-1}\text{s}^{-1})^b$	$k_{\text{HOBr}} (\text{M}^{-1}\text{s}^{-1})^a$
MC-LR	60	61.8	—
MC-RR	58.6	62.2	—
MC-YR	138.6	—	—
MC-LY	92.8	—	—
MC-LW	$\geq 371$	—	—
MC-WR	$\geq 1214$	—	—
MC-LR	—	—	$\geq 6350$

<sup>a</sup> Determined in this work.

<sup>b</sup> Reference (Acero et al., 2005).

the toxicity of algal-impacted waters under various initial  $\text{Br}^-$  concentrations was evaluated by CHO cell chronic cytotoxicity assay. Figs. S7–12 of supplementary material show the concentration-response curves for each sample. The data demonstrated that every sample induced mammalian cell cytotoxicity and generated a significant difference from their concurrent negative control (Table 2). However, to determine if there was a significant difference among the algal samples, a series of  $\text{LC}_{50}$  values using Bootstrap statistics were converted into cytotoxicity index (CTI) values ( $\text{LC}_{50}^{-1}(10^3)$ ) (Varian, 2005). The mean CTI values were analyzed for significant differences using an ANOVA test statistic with pairwise comparison. This generated a metric in which the larger the number, the greater the cytotoxic potency of the sample.

Fig. 5 shows the cytotoxicity index (i.e., CHO cell chronic cytotoxicity) during chlorination under various initial  $\text{Br}^-$  concentrations. The data demonstrated that the CTI value for the algal-impacted water without chlorination was relatively high for a negative control. Table S4 of supplementary material shows MC concentrations in algal-impacted waters. The concentration of MC-LR is the highest among various species of MCs ( $11.97 \mu\text{g/L}$  for  $2 \text{ mg/L DOC}$ ), which is similar to that reported in literature ( $5 \mu\text{g}$  per  $\text{mg}$  of  $\text{DOC}$ ) (Li et al., 2012). For other types of MCs, concentrations range from  $2.03$  to  $2.67 \mu\text{g/L}$  (except for MC-RR,  $0.59 \mu\text{g/L}$ ). It was reported that MC-LR can express cytotoxicity to CHO cells (Lankoff et al., 2003; Xue et al., 2015). Over 100 different MC variants have been identified to date, yet only six MCs were measured in this study due to the lack of commercially available standards. In addition, other cyanotoxins such as cylindrospermopsin and various neurotoxins have been detected in cyanobacteria (Spoof et al., 2003). Therefore, six measured MCs and other matrix (unknown toxins) were likely to be the main contributor to the toxicity of the unchlorinated algal-impacted waters.

When the algal-impacted waters were chlorinated, the mammalian cell cytotoxicity response increased significantly due to the formation of toxic DBPs (as shown in Figs. 1–4). Meanwhile, the concentrations of MC-LR was reduced to  $0.96 \mu\text{g/L}$ , and other MCs were not detected since chlorine can effectively degrade these toxins (Table 1). Based on protein phosphatase 1 inhibition assay (PPIA), the transformation products of chlorinated algal toxins were found to be non-toxic (Rodríguez et al., 2008). This implies that chlorination would reduce the MC-induced cytotoxicity. Increasing the initial concentrations of  $\text{Br}^-$  from  $0$  to  $800 \mu\text{g/L}$  further decreased the concentration of MC-LR to  $0.15 \mu\text{g/L}$ , which was the higher reaction rate constants of bromine towards MC-LR (Table 1). Therefore, the toxicity of treated waters slightly decreased with increasing initial  $\text{Br}^-$  concentrations. In addition, as the initial  $\text{Br}^-$  concentration increased, the formation of unknown DBPs (i.e., unknown TOX) decreased (Fig. S4 of supplementary material). Our recent study has indicated a correlation between cytotoxicity and unknown TOX for disinfected waters (Ersan et al., 2019b).

When the toxicity of chlorinated algal-impacted waters was compared with tap waters from European countries (EU tap waters in Fig. 5) in the literature (Jeong et al., 2012), the cytotoxicity index of the former one was 2–3 times higher than the median value of the tap water. This may indicate that even though algal-impacted waters form less regulated/identified DBPs, the more unknown DBPs/matrix would account for the higher toxicity index.

### 3.4. CHO cell acute genotoxicity analyses

In addition to the chronic cytotoxicity, the acute genotoxicity of the same samples was evaluated. Figs. S13–18 of supplementary material present the genomic DNA damage analyses. Each sample was analyzed for genomic DNA damage with multiple repeated experiments. The % Tail DNA values for each concentration were

**Table 2**

Comparison of the CHO cell cytotoxicity analyses of the unchlorinated and chlorinated algal-impacted water samples.

Sample No	Br <sup>-</sup> concentration before chlorination (μg/L)	Lowest Cytotoxicity. Concentration Factor <sup>a</sup>	LC <sub>50</sub> (Conc. Factor) <sup>b</sup>	r <sup>2</sup> <sup>c</sup>	ANOVA Test <sup>d</sup>
1	unchlorinated	25	89.60	0.98	F <sub>12, 53</sub> = 178.0; P < 0.001
2	0	5	29.62	0.99	F <sub>12, 50</sub> = 211.6; P < 0.001
3	40	5	37.04	0.99	F <sub>12, 50</sub> = 163.0; P < 0.001
4	200	5	34.21	0.99	F <sub>12, 50</sub> = 194.8; P < 0.001
5	400	10	41.35	0.99	F <sub>12, 50</sub> = 105.8; P < 0.001
6	800	10	42.57	0.98	F <sub>12, 50</sub> = 105.6; P < 0.001

<sup>a</sup> Lowest cytotoxic concentration was the lowest concentration factor of the water sample in the concentration-response curve that induced a statistically significant reduction in cell density as compared to the concurrent negative controls.

<sup>b</sup> The LC<sub>50</sub> value is the concentration of the water sample, determined from a regression analysis of the data, that induced a cell density of 50% as compared to the concurrent negative controls.

<sup>c</sup> R<sup>2</sup> is the coefficient of determination for the regression analysis upon which the LC<sub>50</sub> value was calculated.

<sup>d</sup> The degrees of freedom for the between-groups and residual associated with the calculated F-test result and the resulting probability value.

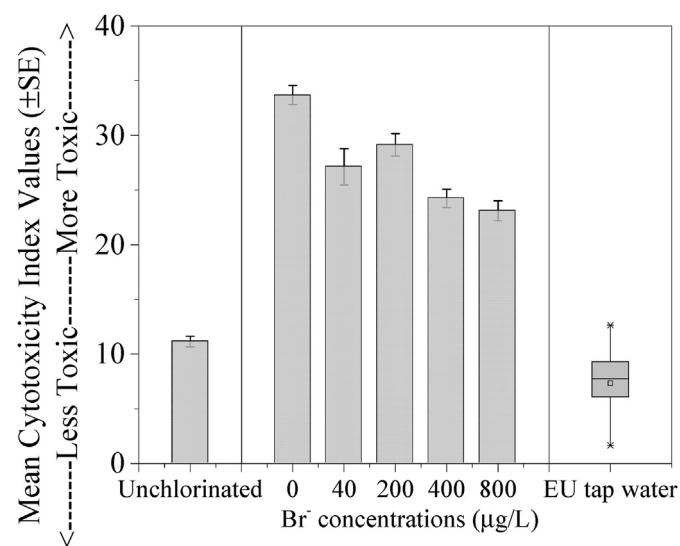


**Fig. 5.** CHO cell cytotoxicity index values for the chlorination of algal-impacted waters under various initial bromide concentrations. Experimental conditions: [DOC] = 2.0 mg C/L, [HOCl]<sub>0</sub> = 4 mg/L, [Br<sup>-</sup>]<sub>0</sub> = 0–800 μg/L, pH = 7.5, T = 21 ± 1 °C, reaction time = 24 h. The data for European country (EU) tap water were from reference (Jeong et al., 2012), where the box shows the 25th percentile, median and 75th percentile. The whisker denotes the 5th and 95th percentile. The symbols “\*” and “□” represent outliers and mean values, respectively.

combined and presented in the concentration-response curves. An analysis of variance test statistic was conducted with the data for each sample (Box et al., 1978). Detailed SCGE analyses for the induction of genomic DNA damage in CHO cells induced by each

sample is presented in Table 3. Fig. 6 shows the CHO cell acute genotoxicity during chlorination of algal-impacted waters under various initial Br<sup>-</sup> concentrations. All samples expressed genotoxicity and generated concentration-response graphs. Due to the

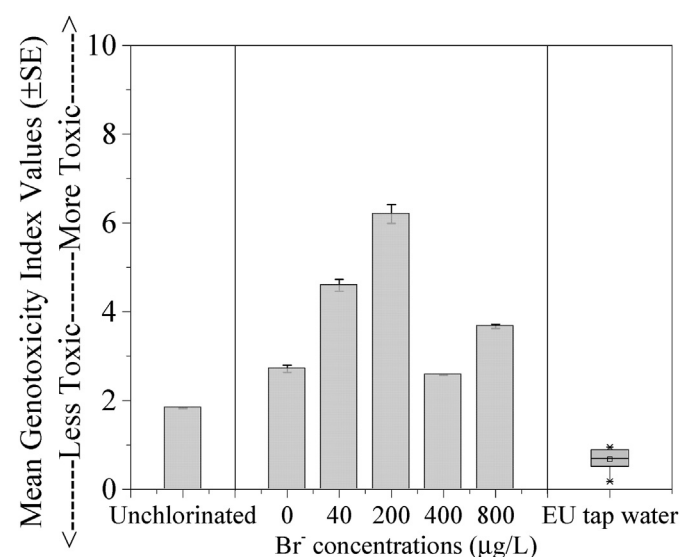


**Fig. 6.** CHO cell genotoxicity index values (±SE) for the chlorination of algal-impacted waters under various initial bromide concentrations. Experimental conditions: [DOC] = 2.0 mg C/L, [HOCl]<sub>0</sub> = 4 mg/L, [Br<sup>-</sup>]<sub>0</sub> = 0–800 μg/L, pH = 7.5, T = 21 ± 1 °C, reaction time = 24 h. The data for EU tap water were from reference (Jeong et al., 2012), where the box shows the 25th percentile, median and 75th percentile. The whisker denotes the 5th and 95th percentile. The symbols “\*” and “□” represent outliers and mean values, respectively.

**Table 3**

CHO cell SCGE genomic DNA damage analyses of the unchlorinated and chlorinated algal-impacted water samples.

Sample No	Br <sup>-</sup> concentration before chlorination (μg/L)	Lowest Genotoxic Conc. Factor <sup>a</sup>	Mean 50% Tail DNA ±SE (Conc. Factor) <sup>b</sup>	r <sup>2</sup> <sup>c</sup>	ANOVA Test Statistic <sup>d</sup>
1	unchlorinated	450	546.7 ± 3.8	0.99	F <sub>8, 27</sub> = 113; P < 0.001
2	0	300	368.5 ± 11.2	0.99	F <sub>5, 16</sub> = 23.0; P < 0.001
3	40	200	217.6 ± 6.2	0.99	F <sub>7, 30</sub> = 83.4; P < 0.001
4	200	100	161.2 ± 5.5	0.99	F <sub>7, 28</sub> = 57.3; P < 0.001
5	400	225	388.2 ± 1.5 ‡	0.95	F <sub>10, 25</sub> = 27.8; P < 0.001
6	800	200	272.3 ± 3.5	0.97	F <sub>9, 30</sub> = 46.4; P < 0.001

<sup>a</sup> Lowest genotoxic concentration was the lowest concentration factor that induced a statistically significant increase in DNA damage as compared to the negative control.

<sup>b</sup> The 50% Tail DNA value is the concentration of the water sample, determined from a regression analysis of the data, that induced a SCGE %T DNA value of 50% as compared to the concurrent negative controls.

<sup>c</sup> r<sup>2</sup> is the coefficient of determination for the regression analysis upon which the 50% Tail DNA value was calculated.

<sup>d</sup> The degrees of freedom for the between-groups and residual associated with the calculated F-test result and the resulting probability value. ‡50% Tail DNA Value extrapolated from the regression analyses of the concentration-response curve.

presence of MCs, unchlorinated algal-impacted waters expressed genotoxicity. Chlorination increased the genotoxicity index, which was attributed to the formation of toxic DBPs. The addition of Br<sup>-</sup> from 40 to 200 µg/L to the algal-impacted waters gradually increased the level of genotoxic response. Samples with initial Br<sup>-</sup> concentrations of 400 and 800 µg/L did not express a continuation of increasing genotoxicity. A possible reason is that further increasing initial concentration of Br<sup>-</sup> did not further remove cyanotoxins (Table S4 of supplementary material), and the genotoxicity was driven preferentially by brominated or nitrogenous species (Plewa et al., 2008). Therefore, the interactions among the cyanotoxins, known DBPs, and unknown DBPs are complex and not dependent on a single set of characteristics. Similarly, the genotoxicity index of chlorinated algal-impacted waters is much higher than that of EU tap waters, the unknown DBPs/matrix in the algal-impacted waters would contribute to the higher toxicity index. Further studies should address the identification of the highly toxic algal-derived by-products.

#### 4. Conclusions

Under practical water treatment conditions, algal-impacted waters produced less regulated THMs, HAAs, HANs, and TOX than NOM. The ratios of DBP from AOM to NOM (median levels) were around 1:5, 1:3, 1:2 and 1:3 for THMs, HAAs, HANs, and TOX, respectively. The second-order rate constant for the reactions of MC-LR with chlorine were  $60 \text{ M}^{-1} \text{ s}^{-1}$  at pH 7.5 and 21 °C, and other variants exhibit comparable or even higher reaction rate constants. The reaction rate constant of bromine with MC-LR is two-orders of magnitude higher than that of chlorine. Owing to the presence of MCs, unchlorinated algal-impacted water expressed toxicity and chlorination further enhanced the mammalian cell cytotoxicity and genotoxicity. Therefore, the observed toxicity of treated waters depended on the evolution of cyanotoxins and the formation of DBPs (particularly unknown or emerging DBPs).

#### Declaration of competing interest

The authors declare that they have no known competing financial interests or personal relationships that could have appeared to influence the work reported in this paper.

#### Acknowledgements

This study was funded, in part, by the National Science Foundation (CBET 1511051). The authors would like to thank Elizabeth Leonard for the kind help on the analyses of microcystins.

#### Appendix A. Supplementary data

Supplementary data to this article can be found online at <https://doi.org/10.1016/j.watres.2020.116145>.

#### References

- Acero, J.L., Rodriguez, E., Meriluoto, J., 2005. Kinetics of reactions between chlorine and the cyanobacterial toxins microcystins. *Water Res.* 39 (8), 1628–1638.
- Box, G.E.P., Hunter, W.G., Hunter, J.S., 1978. *Statistics for Experimenters: an Introduction to Design, Data Analysis, and Model Building*. Wiley & Sons Inc., New York, NY.
- Chapra, S.C., Boehlert, B., Fant, C., Bierman, V.J., Henderson, J., Mills, D., Mas, D.M.L., Rennels, L., Jantarasami, L., Martinich, J., Strzepke, K.M., Paerl, H.W., 2017. Climate change impacts on harmful algal blooms in U.S. Freshwaters: a screening-level assessment. *Environ. Sci. Technol.* 51 (16), 8933–8943.
- Dawson, R.M., 1998. The toxicology of microcystins. *Toxicol.* 36 (7), 953–962.
- Deborde, M., von Gunten, U., 2008. Reactions of chlorine with inorganic and organic compounds during water treatment - kinetics and mechanisms: a critical review. *Water Res.* 42 (1–2), 13–51.
- Ersan, M.S., Liu, C., Amy, G., Karanfil, T., 2019a. The interplay between natural organic matter and bromide on bromine substitution. *Sci. Total Environ.* 646, 1172–1181.
- Ersan, M.S., Liu, C., Amy, G., Plewa, M.J., Wagner, E.D., Karanfil, T., 2019b. Chloramination of iodide-containing waters: formation of iodinated disinfection byproducts and toxicity correlation with total organic halides of treated waters. *Sci. Total Environ.* 697, 134142.
- Fairbairn, D.W., Olive, P.L., O'Neill, K.L., 1995. The comet assay: a comprehensive review. *Mutat. Res.* 339 (1), 37–59.
- Fang, J., Yang, X., Ma, J., Shang, C., Zhao, Q., 2010. Characterization of algal organic matter and formation of DBPs from chlor(am)ination. *Water Res.* 44 (20), 5897–5906.
- Good, K.D., VanBriesen, J.M., 2016. Current and potential future bromide loads from coal-fired power plants in the allegheny river basin and their effects on downstream concentrations. *Environ. Sci. Technol.* 50 (17), 9078–9088.
- Heeb, M.B., Criquet, J., Zimmermann-Steffens, S.G., von Gunten, U., 2014. Bromine production during oxidative water treatment of bromide-containing waters and its reactions with inorganic and organic compounds: a critical review. *Water Res.* 48 (1), 15–42.
- Henderson, R.K., Baker, A., Parsons, S.A., Jefferson, B., 2008. Characterisation of algogenic organic matter extracted from cyanobacteria, green algae and diatoms. *Water Res.* 42 (13), 3435–3445.
- Her, N., Amy, G., Park, H.-R., Song, M., 2004. Characterizing algogenic organic matter (AOM) and evaluating associated NF membrane fouling. *Water Res.* 38 (6), 1427–1438.
- Himberg, K., Keijola, A.M., Hiisvirta, L., Pyysalo, H., Sivonen, K., 1989. The effect of water treatment processes on the removal of hepatotoxins from *Microcystis* and *Oscillatoria* cyanobacteria: a laboratory study. *Water Res.* 23 (8), 979–984.
- Ho, L., Onstad, G., von Gunten, U., Rinck-Pfeiffer, S., Craig, K., Newcombe, G., 2006. Differences in the chlorine reactivity of four microcystin analogues. *Water Res.* 40 (6), 1200–1209.
- Hu, J., Song, H., Karanfil, T., 2010. Comparative analysis of halonitromethane and trihalomethane formation and speciation in drinking water: the effects of disinfectants, pH, bromide, and nitrite. *Environ. Sci. Technol.* 44 (2), 794–799.
- Hua, G., Reckhow, D.A., Kim, J., 2006. Effect of bromide and iodide ions on the formation and speciation of disinfection by-products during chlorination. *Environ. Sci. Technol.* 40, 3050–3056.
- Hureiki, L., Croue, J.-P., Legube, B., 1994. Chlorination studies of free and combined amino acids. *Water Res.* 28, 2521.
- Jeong, C.H., Wagner, E.D., Siebert, V.R., Anduri, S., Richardson, S.D., Daiber, E.J., McKague, A.B., Kogevinas, M., Villanueva, C.M., Goslan, E.H., Luo, W., Isabelle, L.M., Pankow, J.F., Grazuleviciene, R., Cordier, S., Edwards, S.C., Righi, E., Nieuwenhuijsen, M.J., Plewa, M.J., 2012. Occurrence and toxicity of disinfection byproducts in european drinking waters in relation with the HIWATE epidemiology study. *Environ. Sci. Technol.* 46 (21), 12120–12128.
- Kim, D., Amy, G.L., Karanfil, T., 2015. Disinfection by-product formation during seawater desalination: a review. *Water Res.* 81, 343–355, 0.
- Kristiana, I., Lethorn, A., Joll, C., Heitz, A., 2014. To add or not to add: the use of quenching agents for the analysis of disinfection by-products in water samples. *Water Res.* 59, 90–98.
- Kumaravel, T.S., Jha, A.N., 2006. Reliable Comet assay measurements for detecting DNA damage induced by ionising radiation and chemicals. *Mutat. Res.* 605 (1–2), 7–16.
- Lankoff, A., Banasik, A., Obe, G., Deperas, M., Kuzminski, K., Tarczynska, M., Jurczak, T., Wojcik, A., 2003. Effect of microcystin-LR and cyanobacterial extract from polish reservoir of drinking water on cell cycle progression, mitotic spindle, and apoptosis in CHO-K1 cells. *Toxicol. Appl. Pharmacol.* 189 (3), 204–213.
- Lee, W., Westerhoff, P., 2006. Dissolved organic nitrogen removal during water treatment by aluminum sulfate and cationic polymer coagulation. *Water Res.* 40 (20), 3767–3774.
- Leenheer, J.A., Croue, J.-P., 2003. Peer reviewed: characterizing aquatic dissolved organic matter. *Environ. Sci. Technol.* 37 (1), 18A–26A.
- Li, L., Gao, N., Deng, Y., Yao, J., Zhang, K., 2012. Characterization of intracellular & extracellular algae organic matters (AOM) of *Microcystis aeruginosa* and formation of AOM-associated disinfection byproducts and odor & taste compounds. *Water Res.* 46 (4), 1233–1240.
- Liu, C., Croue, J.-P., 2016. Formation of bromate and halogenated disinfection byproducts during chlorination of bromide-containing waters in the presence of dissolved organic matter and CuO. *Environ. Sci. Technol.* 50 (1), 135–144.
- Liu, C., Ersan, M.S., Plewa, M.J., Amy, G., Karanfil, T., 2018. Formation of regulated and unregulated disinfection byproducts during chlorination of algal organic matter extracted from freshwater and marine algae. *Water Res.* 142, 313–324.
- Liu, C., Ersan, M.S., Plewa, M.J., Amy, G., Karanfil, T., 2019. Formation of iodinated trihalomethanes and noniodinated disinfection byproducts during chloramination of algal organic matter extracted from *Microcystis aeruginosa*. *Water Res.* 162, 115–126.
- Liu, C., Olivares, C.I., Pinto, A.J., Lauderdale, C.V., Brown, J., Selbes, M., Karanfil, T., 2017. The control of disinfection byproducts and their precursors in biologically active filtration processes. *Water Res.* 124, 630–653.
- Liu, C., von Gunten, U., Croue, J.-P., 2012. Enhanced bromate formation during chlorination of bromide-containing waters in the presence of CuO: catalytic disproportionation of hypobromous acid. *Environ. Sci. Technol.* 46 (20), 11054–11061.
- Merel, S., Clément, M., Thomas, O., 2010. State of the art on cyanotoxins in water



- and their behaviour towards chlorine. *Toxicon* 55 (4), 677–691.
- Paerl, H.W., Huisman, J., 2008. Blooms like it hot. *Science* 320 (5872), 57–58.
- Pattison, D.I., Hawkins, C.L., Davies, M.J., 2007. Hypochlorous acid-mediated protein Oxidation: how important are chloramine transfer reactions and protein tertiary structure? *Biochemistry* 46 (34), 9853–9864.
- Plewa, M.J., 2016. XAD-2/XAD-8 Resin Preparation, Column Construction and Regeneration: SOP. University of Illinois at Urbana-Champaign, Urbana.
- Plewa, M.J., Wagner, E.D., Muellner, M.G., Hsu, K.M., Richardson, S.D., 2008. Comparative mammalian cell toxicity of N-DBPs and C-DBPs. In: Karanfil, T., Krasner, S.W., Westerhoff, P., Xie, Y. (Eds.), *Occurrence, Formation, Health Effects and Control of Disinfection By-Products in Drinking Water*. American Chemical Society, Washington, D.C., pp. 36–50.
- Plewa, M.J., Wagner, E.D., Richardson, S.D., 2017. TIC-Tox: a preliminary discussion on identifying the forcing agents of DBP-mediated toxicity of disinfected water. *J. Environ. Sci.* 58, 208–216.
- Plewa, M.J., Wagner, E.D., Richardson, S.D., Thruston, A.D., Woo, Y.T., McKague, A.B., 2004. Chemical and biological characterization of newly discovered iodoacid drinking water disinfection byproducts. *Environ. Sci. Technol.* 38 (18), 4713–4722.
- Qi, J., Lan, H., Liu, R., Miao, S., Liu, H., Qu, J., 2016. Prechlorination of algae-laden water: the effects of transportation time on cell integrity, algal organic matter release, and chlorinated disinfection byproduct formation. *Water Res.* 102, 221–228.
- Rinehart, K.L., Harada, K., Namikoshi, M., Chen, C., Harvis, C.A., Munro, M.H.G., Blunt, J.W., Mulligan, P.E., Beasley, V.R., et al., 1988. Nodularin, microcystin, and the configuration of Adda. *J. Am. Chem. Soc.* 110 (25), 8557–8558.
- Rodríguez, E.M., Acero, J.L., Spoo, L., Meriluoto, J., 2008. Oxidation of MC-LR and -RR with chlorine and potassium permanganate: toxicity of the reaction products. *Water Res.* 42 (6), 1744–1752.
- Rodríguez, E., Onstad, G.D., Kull, T.P.J., Metcalf, J.S., Acero, J.L., von Gunten, U., 2007. Oxidative elimination of cyanotoxins: comparison of ozone, chlorine, chlorine dioxide and permanganate. *Water Res.* 41 (15), 3381–3393.
- Rundell, M.S., Wagner, E.D., Plewa, M.J., 2003. The comet assay: genotoxic damage or nuclear fragmentation? *Environ. Mol. Mutagen.* 42 (2), 61–67.
- Selbes, M., Shan, J., Bekaroglu, S.S.K., Karanfil, T., 2015. Recent Advances in Disinfection By-Products. American Chemical Society, pp. 215–234.
- Spoo, L., Vesterkvist, P., Lindholm, T., Meriluoto, J., 2003. Screening for cyanobacterial hepatotoxins, microcystins and nodularin in environmental water samples by reversed-phase liquid chromatography–electrospray ionisation mass spectrometry. *J. Chromatogr. A* 1020 (1), 105–119.
- Tice, R.R., Agurell, E., Anderson, D., Burlinson, B., Hartmann, A., Kobayashi, H., Miyamae, Y., Rojas, E., Ryu, J.C., Sasaki, Y.F., 2000. Single cell gel/comet assay: guidelines for in vitro and in vivo genetic toxicology testing. *Environ. Mol. Mutagen.* 35 (3), 206–221.
- U.S. Environmental Protection Agency, 2006. National Primary Drinking Water Regulations. Stage 2 disinfectants and disinfection byproducts rule; final rule. Fed. Regist. Part II 71 (2), 388–493, 40 CFR Parts 9, 141, and 142, Washington D.C.
- Varian, H., 2005. Bootstrap tutorial. *Math. J.* 9, 768–775.
- Wagner, E.D., Plewa, M.J., 2009. In: Dhawan, A., Anderson, D. (Eds.), *The Comet Assay in Toxicology*. Royal Society of Chemistry, London, pp. 79–97.
- Wagner, E.D., Plewa, M.J., 2017. CHO cell cytotoxicity and genotoxicity analyses of disinfection by-products: an updated review. *J. Environ. Sci.* 58, 64–76.
- Widrig, D.L., Gray, K.A., McAuliffe, K.S., 1996. Removal of algal-derived organic material by preozonation and coagulation: monitoring changes in organic quality by pyrolysis-GC-MS. *Water Res.* 30 (11), 2621–2632.
- World Health Organization, 2011. *Guidelines for Drinking-Water Quality*, Geneva.
- Xiang, L., Li, Y.-W., Liu, B.-L., Zhao, H.-M., Li, H., Cai, Q.-Y., Mo, C.-H., Wong, M.-H., Li, Q.X., 2019. High ecological and human health risks from microcystins in vegetable fields in southern China. *Environ. Int.* 133, 105142.
- Xue, L., Li, J., Li, Y., Chu, C., Xie, G., Qin, J., Yang, M., Zhuang, D., Cui, L., Zhang, H., Fu, X., 2015. N-acetylcysteine protects Chinese Hamster ovary cells from oxidative injury and apoptosis induced by microcystin-LR. *Int. J. Clin. Exp. Med.* 8 (4), 4911–4921.
- Yoshizawa, S., Matsushima, R., Watanabe, M.F., Harada, K.-i., Ichihara, A., Carmichael, W.W., Fujiki, H., 1990. Inhibition of protein phosphatases by microcystins and nodularin associated with hepatotoxicity. *J. Canc. Res. Clin. Oncol.* 116 (6), 609–614.